

# Nanosized manganese oxide as cathode material for lithium batteries: Influence of carbon mixing and grinding on cyclability

A. Ibarra-Palos<sup>a,\*</sup>, P. Strobel<sup>a</sup>, C. Darie<sup>a</sup>, M. Bacia<sup>a</sup>, J.B. Soupart<sup>b</sup>

<sup>a</sup> Centre National de la Recherche Scientifique, Laboratoire de Cristallographie, BP166, 38042 Grenoble Cedex 9, France

<sup>b</sup> Erachem-Comilog, B-7333 Tertre, Belgium

Available online 31 May 2005

## Abstract

New manganese oxo-iodides were prepared by redox reaction of sodium permanganate with lithium iodide in aqueous medium at room temperature. The effects of Li/Mn ratio, carbon incorporation at the synthesis stage and grinding were systematically studied. Structural characterization showed that these materials are nanocrystalline. Best electrochemical results were obtained either on samples with carbon mixed after synthesized, submitted to extensive grinding before electrode fabrication, or on samples for which carbon black was incorporated directly in the aqueous reaction medium at the synthesis stage. Typical capacities in the potential window 1.8–3.8 V are 160 and 130 mAh g<sup>-1</sup> at the 40th and 100th cycle, respectively.

© 2005 Published by Elsevier B.V.

**Keywords:** Lithium batteries; Manganese oxide; Nanocrystalline oxide

## 1. Introduction

In the last few years, several amorphous phases, principally manganese oxides, have been proposed as positive electrode materials for lithium batteries. Most of them have been prepared with permanganates as raw material, using several reducing agents, for instance oxalic acid [1], fumaric acid [2] or potassium borohydride [3]. The most promising of these materials is an oxo-iodide proposed by Kim and Manthiram [4,5], which showed capacities in excess of 200 mAh g<sup>-1</sup> at the 40th cycle (in the potential window 1.5–4.5 V) and no significant tendency to convert into spinel. Peculiarities of Kim and Manthiram's route include: (i) the use of lithium iodide as a reducing agent and (ii) a synthesis process completely excluding water. The latter aspect is a serious drawback in view of practical applications. In addition, a more recent report on this oxo-iodide showed capacities of only ca. 120 mAh g<sup>-1</sup> within limits 2–4 V [6]. We have recently investigated the synthesis of disordered lithium/sodium man-

ganates using the chemical reaction of sodium permanganate with various reducing reagents (chloride, iodide, hydrogen peroxide or oxalate) in aqueous solution [7]. These yielded hydrated oxides with Mn valence in the range 3.80–3.92 and a much lower alkali cation content than Kim and Manthiram's. Among these compounds, the one obtained by reduction with iodide shows remarkable properties. It is the easiest to dehydrate at moderate temperature (240 °C) and shows the best electrochemical behaviour an initial capacity >170 Ah kg<sup>-1</sup>, slowly decreasing on cycling to reach 140 Ah kg<sup>-1</sup> after 70 cycles (1.8–3.8 V potential window).

Manganese oxides are known not to be good electric conductors, and the addition of conducting carbon is a key step in the fabrication of suitable electrodes for lithium batteries. Remarkable improvements in battery performance have been obtained recently by including carbon black at the oxide synthesis stage instead of the usual process of mixing carbon with pre-synthesized electrode material. For instance, an increase in cycling capacity of LiMn<sub>2</sub>O<sub>4</sub> spinel has been reported when carbon black was included during the oxide preparation process [8,9]. A similar technique was used for an amorphous oxide obtained by decomposition of potassium permanganate [9].

\* Corresponding author. Present address: Instituto de Investigaciones en Materiales, Universidad Nacional Autónoma de México, A.P. 70-360, Ciudad Universitaria, Coyoacan 04510, México, D.F., Mexico.

Grain size is another factor playing an important role in the performance of lithium battery materials. In the case of  $\text{LiMn}_2\text{O}_4$ , several studies found a relationship between grain size and electrochemical performances. Samples with small grain size can be obtained by co-precipitation [10] or via sol–gel [11]. A remarkable cycling stability has been reported for  $\text{LiMn}_2\text{O}_4$  after extended mechanical grinding [12].

We present here the results of a detailed study of the manganese oxides obtained by the aqueous permanganate-iodide route, focusing on the influence of: (i) the inclusion of conducting carbon at an early stage of the electrode preparation, (ii) mechanical grinding and (iii) the initial Li/Mn ratio. Samples with remarkable stability on cycling (ca. 130 mAh  $\text{g}^{-1}$  after 100 cycles) were obtained by optimizing these factors.

## 2. Experimental

The synthesis procedure was based on that described previously [7]. The starting material was a 0.5 M aqueous solution of sodium permanganate (Aldrich). All reactions were carried out in at least a six-fold excess  $\text{Li}^+$  (aqueous LiI solution) with respect to  $\text{NaMnO}_4$  concentration, at room temperature under vigorous stirring for 15 h. In the case of samples including carbon black at the synthesis stage, 250 mg of carbon black (Y50A grade, SNNA, Berre, France) was added to the LiI solution under stirring. Products were washed with distilled water, filtered and dried at 80 °C in air.

Samples were characterised by X-ray diffraction using a Siemens D-5000 diffractometer (Cu  $K\alpha$  radiation), scanning (JEOL 840) and transmission electron microscopy (Philips CM300). Chemical compositions were determined by atomic absorption spectrophotometry for Li, Na and Mn contents and standard oxalate/permanganate volumetric titration for manganese oxidation state. Iodine/manganese ratios were obtained from EDX measurements coupled to SEM.

For positive electrode preparation, the oxide was intimately mixed with carbon black (for those samples where carbon was not added earlier) and PTFE emulsion in weight ratio 70:20:10. The effect of additional grinding was studied on oxide–carbon mixtures subjected to mechanical grinding in a rotary mixer/grinder Retsch RM 100 where mixtures were subjected to grinding at 150 rpm for 15 or 60 min.

Electrochemical tests were carried out in liquid electrolyte at room temperature using Swagelok-type batteries at room temperature. The positive mixture paste was rolled down to 0.1 mm thickness, cut into pellets with diameter 10 mm and dried at 120 °C under vacuum. Typical active material weights used were 6–12 mg  $\text{cm}^2$ . The electrolyte was a 1 M solution of  $\text{LiPF}_6$  in EC-DMC 1:2. Negative electrodes were 200  $\mu\text{m}$ -thick lithium foil (Metall Ges., Germany). Cells were assembled in a glove box under argon with  $\leq 1$  ppm  $\text{H}_2\text{O}$ . Electrochemical studies were carried out using a MacPile Controller (Bio-Logic, Claix, France) in galvanostatic mode in the potential window 1.8–3.8 V (up to 4.2 V in some cases).

## 3. Results and discussion

### 3.1. Synthesis and composition

The syntheses conditions and analysis results are given in Table 1. All samples have an alkali metal/Mn ratio in the range 0.53–0.63 with  $\text{Na} \leq 0.10$  except sample A, containing more sodium. Note that these ratios are much smaller than those reported for syntheses in non-aqueous medium [4]. The oxidation state determination gave results in excess of  $\text{Mn}^{4+}$ , which can be explained by the contribution of iodine. Hwang et al. [13] recently showed that iodine species in such manganese ‘oxi-iodides’ prepared in aqueous medium are most likely iodate anions  $\text{IO}_3^-$ . These obviously participate in the redox titration, where their contribution cannot be separated from that of manganese. The iodine fraction could not be determined with great accuracy (see Table 1); however, a combination of the total oxidizing power and iodine concentration yields manganese valence close to 4 in all samples. The quantity of LiI was purposely increased in sample E in order to increase the iodine concentration in the final sample; no significantly larger iodine content resulted.

### 3.2. Physico-chemical characterization

The specific surface area of these oxides is in the range 20–40  $\text{m}^2 \text{g}^{-1}$ . They give no significant XRD peaks, indicating either an amorphous character or a grain size smaller than the coherence length of the X-ray beam. SEM analysis on the composite films including carbon black and PTFE. It shows that mechanical grinding has an important effect on the particle size. Before grinding, the grain size is rather heterogeneous and contains particles up to 50  $\mu\text{m}$ . Grinding reduces the grain size to the micrometer range and also improves homogeneity (see Fig. 1). SEM observation also shows that incorporation of carbon black at the synthesis stage improves significantly the quality and homogeneity of carbon distribution in the oxide.

Transmission electron microscopy shows that the actual crystallites are much smaller and that the material gives diffraction rings (see Fig. 2). This gives evidence that these materials are not amorphous, but *nanocrystalline*. The structural characterization of these materials, including electron diffraction and X-ray absorption spectroscopy at the

Table 1  
Syntheses conditions and analyses

Sample	Carbon in reaction medium	Li/Mn in reaction medium	Cationic formula	Iodine <sup>a</sup> (mol%)
A	No	≈6	$\text{Li}_{0.38}\text{Na}_{0.22}\text{MnO}_x$	1
B	Yes	≈6	$\text{Li}_{0.46}\text{Na}_{0.07}\text{MnO}_x$	2
C	No	10.6	$\text{Li}_{0.53}\text{Na}_{0.06}\text{MnO}_x$	4
D	Yes	10.4	$\text{Li}_{0.55}\text{Na}_{0.08}\text{MnO}_x$	4
E	No	11.9	Not determined	3

<sup>a</sup> Approximate EDAX analysis on powder samples.

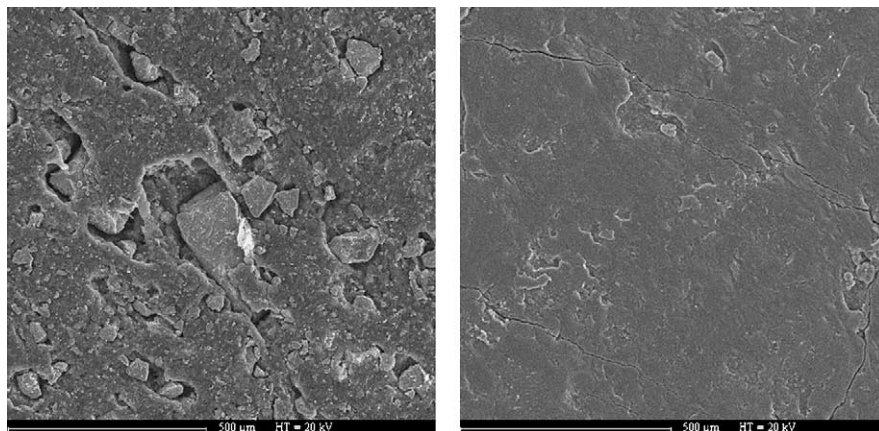


Fig. 1. SEM pictures of sample C. Left: initial sample; right: after 60 min grinding (the scale is 1 mm full width in both figures).

manganese edge will be addressed in more detail elsewhere [14].

### 3.3. Electrochemical behaviour

Fig. 3 shows the first discharge–charge cycle of samples A–D, as prepared. All samples give smooth, reversible S-shaped discharge–charge curve with the main discharge plateau at 2.8–2.9 V, in agreement with previous studies [4,7]. The charge–discharge curve shape does not change significantly on cycling, and differs considerably from the behaviour of long-range 2D or 3D manganese oxide networks such as spinel or  $\text{LiMnO}_2$ . No evidence of conversion to spinel was found, even after more than 100 cycles.

#### 3.3.1. Effect of carbon addition procedure

Fig. 3 shows significant differences in the cycling curves depending whether or not carbon black was included at the synthesis stage or not. Whereas samples B and D (carbon in-

cluded) have first cycle capacities in excess of  $150 \text{ mAh g}^{-1}$ , the 2.8 V plateau is interrupted much earlier in samples where carbon was added at a later stage (samples A and C). For these samples, we also note a large increase in voltage during relaxation at the end of discharge: the cell potential goes back up to 2.40–2.45 V for both A and C within 3 h, compared to 2.07 V for samples B and D. This relaxation behaviour shows that the mixture with carbon mixed after synthesis is unsatisfactory, and that the reduction process during discharge in samples A and C is probably hindered by bad inter-grain conduction, leaving a significant fraction of the positive electrode unused.

Fig. 4 shows the evolution of the capacities of samples C and D with cycling. The capacity is rather stable in both cases, and remains much higher for sample D ( $160 \text{ mAh g}^{-1}$  at the 40th cycle). Note that the average capacity is not observed at the first discharge. We attribute this to the fact that the valence of Mn is lower than 4 in the initial material, and that the presence of lithium makes it possible to push the lithium deintercalation on charge to a higher valence and lower lithium content than in the initial material. This effect

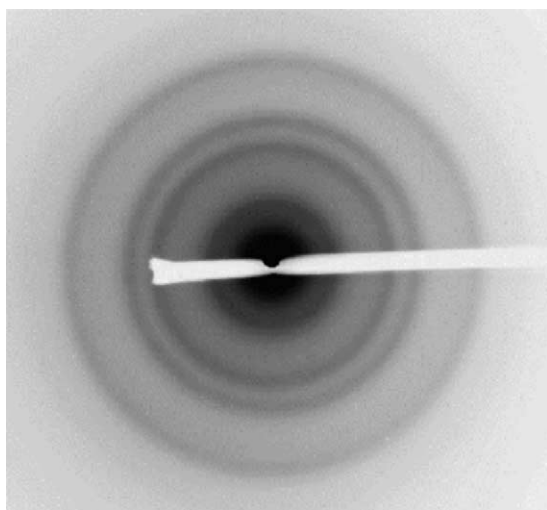


Fig. 2. Electron diffraction diagram of a nanosized sample obtained by the aqueous  $\text{NaMnO}_4$ –LiI process.

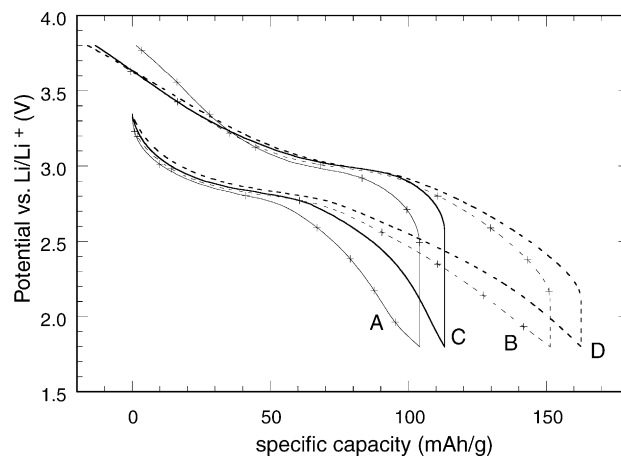


Fig. 3. First discharge–charge cycle of samples A–D. Conditions: room temperature, voltage window 1.8–3.8 V, discharge regime C/18–C/20 (for 1 Li/Mn).

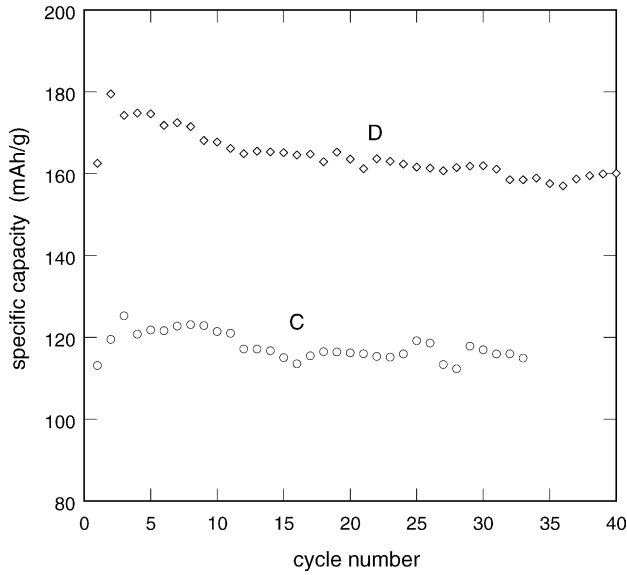


Fig. 4. Evolution of capacity with cycle number for samples C (carbon added after synthesis) and D (carbon added at synthesis stage). Cycling conditions are as in Fig. 4.

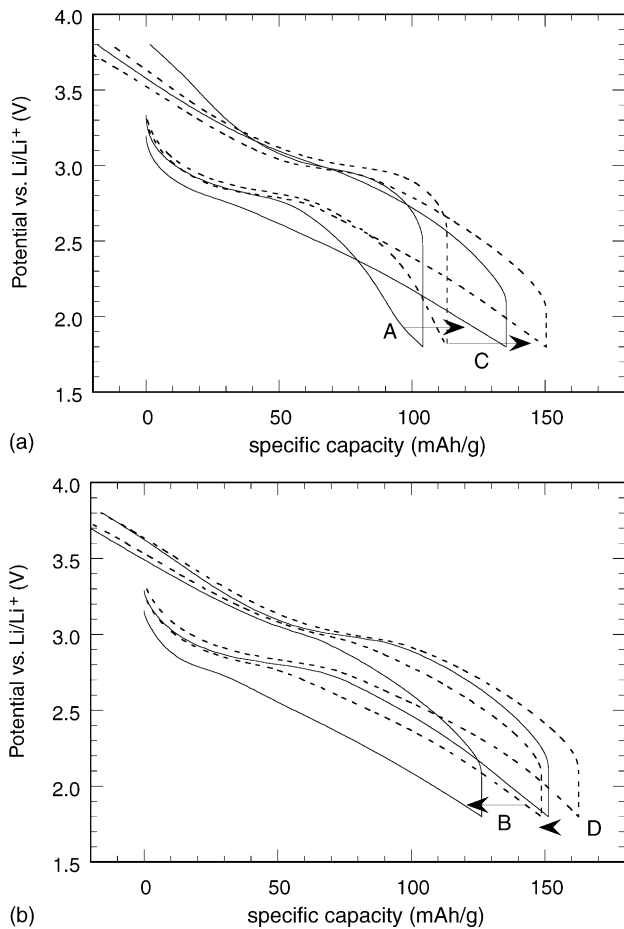


Fig. 5. Comparing the first discharge–charge cycling of samples A–D before and after grinding (same conditions as in Fig. 1. (a) Carbon mixed after synthesis and (b) carbon added at the synthesis stage. The arrows show the evolution from non-ground to ground samples.

is clearly visible for all battery cyclings (see more examples in Fig. 6, for instance).

3.3.2. Effect of grinding

Turning now to grinding, Fig. 6 shows a remarkably different effect depending on incorporation of carbon black after or during the synthesis of the oxide. In the former case (Fig. 5a), a 60 min grinding increases significantly the capacity, whereas the opposite effect is observed in the latter (Fig. 5b). This trend applies for all samples, and determines the performance of the electrode material not only in the initial cycle, but on extended cycling as well, as shown in Fig. 6. The main effect is obtained within 15 min grinding and is quite spectacular: the capacity of non-ground sample C jumps from ca. 120 to 160 mAh h<sup>-1</sup> after 15 min grinding, and becomes very similar to that of not-ground sample D after 60 min grinding.

The effect of grinding on electrochemical performances can be explained as follows. As already shown by the limited discharge plateau length and high voltage change on relaxation at end of discharge, the capacity of samples with carbon added by post-synthesis mixing is rather poor due to bad oxide–carbon grain contact. Grinding reduces the grain

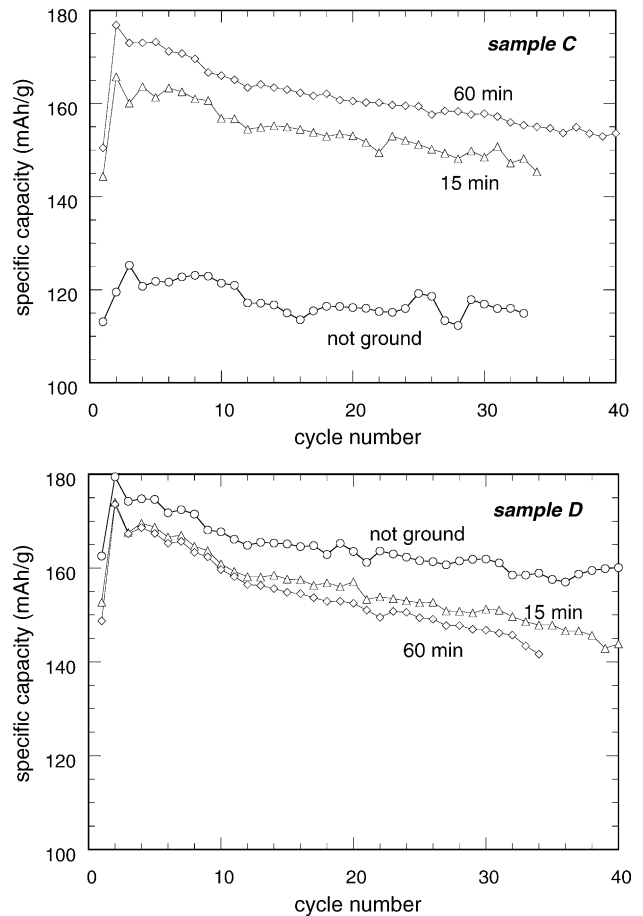


Fig. 6. Evolution of capacity of samples C (top) and D (bottom) as a function of cycling for different grinding times. Cycling conditions are as in Fig. 4.

size and improves the contact between oxide and carbon grains, thereby increasing the electrochemical capacity. In samples with carbon included at the synthesis stage, on the contrary, grains are much smaller and the contact between oxide and carbon grains much more intimate. In this case, the grain size is not improved by grinding and we suspect that grinding shocks partially break the oxide–carbon contacts. In summary, good cycling performances are obtained either

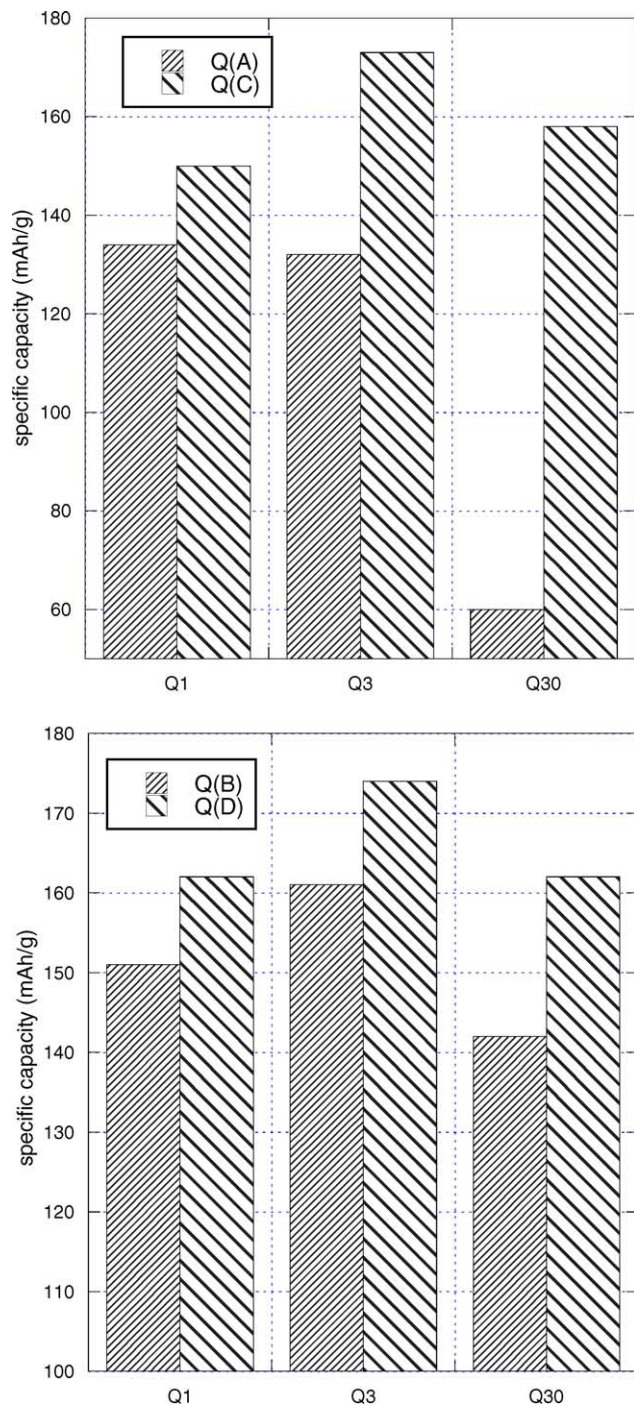


Fig. 7. Comparing the discharge capacities at 1st ( $Q_1$ ), 10th ( $Q_{10}$ ) and 30th ( $Q_{30}$ ) cycle for optimized samples A–C (top) and B–D (bottom).

on samples with carbon included in the synthesis without further grinding, or on samples with carbon added later and ground.

### 3.3.3. Effect of chemical composition

A last experimental parameter was varied in this study: the composition of the reaction medium and hence of the material obtained. The trends outlined above distinguished only two sets: samples with carbon added at the synthesis stage (B and D, not distinguished so far) and samples with carbon mixed later (A and C). A more detailed analysis of the capacity values in the optimized materials (either carbon included—without grinding, or carbon added later + grinding) gives results shown as histograms in Fig. 7. In both sets, the sample with higher Li/Mn ratio and higher iodine content (C and D in Table 1) systematically yielded better cycling performances. It should be pointed out that the iodine content could not be increased further; electrochemical tests on sample E, intended to increase further the iodine content, but without success, were actually poorer than those for samples C or D. Other studies also concluded to a very limited concentration range of iodine in such oxides [14].

### 3.3.4. Extended cycling capacity

The batteries with best characteristics, i.e. made from sample C with grinding or from sample D without grinding were subjected to extended cycling. Fig. 8 shows results of cycling up to 100 cycles for such batteries. The capacities of these two materials are very similar. They remain high ( $160 \text{ mAh g}^{-1}$ ) up to ca. 40 cycles, and decrease slowly but constantly on further cycling. It is, however, higher than that of manganese spinels, which behave very poorly in the same potential range (1.8–3.8 V used here). We believe that this decrease is mostly due to inter-grain conductivity problems, and that it could be reduced by specific coating or carbon mixing optimization processes.

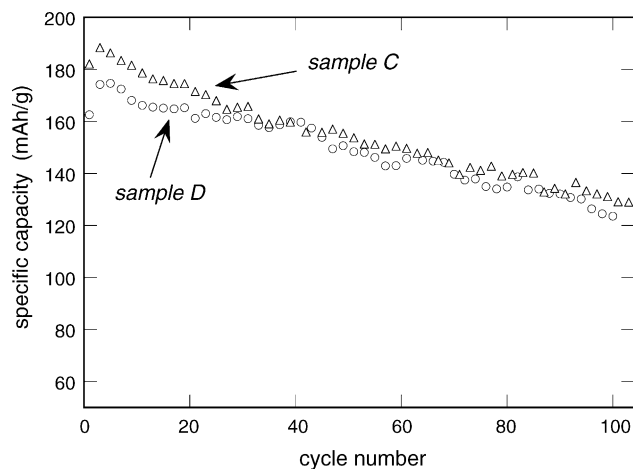


Fig. 8. Evolution of capacity of optimized samples C (carbon mixed after preparation, with grinding) and D (carbon included in synthesis stage, no grinding) at C/20 (referring to 1 Li/Mn) in potential window 1.8–3.8 V.

#### 4. Conclusions

In this study, we investigated nanocrystalline manganese oxo-iodides as positive electrode materials for lithium batteries. The intrinsic capacity of these materials is high ( $>160 \text{ mAh g}^{-1}$ ). Systematic studies show that this intrinsic capacity can be reached either by incorporating the carbon black conducting additive at the synthesis step, or by extended grinding of the oxide–carbon mixture. These materials exhibit moderate fading on cycling and do not show any tendency toward spinel formation, unlike many other disordered manganese oxides, and thus constitute interesting candidates for lithium batteries.

#### References

- [1] F. Leroux, L.F. Nazar, *Solid State Ionics* 100 (1997) 103.
- [2] J.J. Xu, A.J. Kinser, B.B. Owens, W.H. Smyrl, *Electrochem. Solid State Lett.* 1 (1998) 1.
- [3] C. Tsang, J. Kim, A. Manthiram, *J. Solid State Chem.* 137 (1998) 28.
- [4] J. Kim, A. Manthiram, *Nature* 390 (1997) 265.
- [5] J. Kim, A. Manthiram, *Electrochem. Solid State Lett.* 2 (1999) 55.
- [6] C.R. Horne, U. Bergmann, J. Kim, K.A. Striebel, A. Manthiram, S.P. Cramer, E.J. Cairns, *J. Electrochem. Soc.* 147 (2000) 395.
- [7] A. Ibarra-Palos, M. Anne, P. Strobel, *Solid State Ionics* 138 (2001) 203.
- [8] H. Huang, *J. Power Sources* 54 (1995) 319.
- [9] P. Bezdicka, T. Grygar, B. Klápěte, J. Vondrák, *Electrochim. Acta* 45 (1999) 913.
- [10] N. Treuil, C. Labrugere, M. Ménétrier, J. Portier, G. Campet, S.J. Hwang, S.W. Song, J.H. Choy, *J. Phys. Chem. B* 103 (1999) 2100.
- [11] J.H. Choy, D.H. Kim, C.W. Kwon, S.J. Hwang, Y.I. Kim, *J. Power Sources* 77 (1999) 1.
- [12] S.H. Kang, J.B. Goodenough, L.K. Rabenberg, *Electrochem. Solid State Lett.* 4 (2001) 49.
- [13] S.J. Hwang, C.W. Kwon, G. Campet, J.H. Choy, *Electrochem. Solid State Lett.* 7 (2004) 49.
- [14] P. Strobel, A. Ibarra-Palos, C. Darie, M. Bacia, J.B. Soupart, *Chem. Mater.* (submitted).